# Adaptive wall treatment for the elliptic blending Reynolds stress model

Jean-François Wald, Sofiane Benhamadouche, Remi Manceau

# ADAPTIVE WALL TREATMENT FOR THE ELLIPTIC BLENDING REYNOLDS STRESS MODEL

***Jean-Francois Wald*[1,2], *Sofiane Benhamadouche*[1] *and Rémi Manceau*[2]**

[1] ***EDF R&D, Fluid Mechanics, Energy and Environment Dept., 6 quai Watier, 78401 Chatou, France***

[2] ***Departement of applied mathematics, CNRS-University of Pau-Inria, IPRA, avenue de l'université, 64013 Pau, France***

**jean-francois.wald@edf.fr**

## 1 Introduction

Wall functions are widely used in CFD in order to significantly reduce the computational cost compared to so called Low-Reynolds number formulations. They are, however, particularly restrictive in terms of meshing as they require the first calculation point to fall into the logarithmic region. Industrial simulations of internal flows, such as the ones encountered in nuclear applications, are particularly challenging due to their inherent complexity that makes it difficult to satisfy those conditions everywhere.

Several proposals were formulated in the literature that aim at improving and generalizing wall treatments. Chieng and Launder [1] improve the classical wall function strategy by accounting for a linear variation of the shear stress and the turbulent kinetic energy in the first near wall cell. A more general formulation of this strategy was developed by Craft *et al.* [2], who derive Wall Functions (WFs) on the basis of an assumed eddy viscosity distribution through this cell. A refined approach, also due to Craft *et al.* [3], proposes the integration all the simplified transport equations over a fine embedded subgrid within the first cell. Kalitzin [4] developed an adaptive strategy based on curve-fitting of the variables using splines.

Another strategy, widely used in CFD, consists in using a blending of the wall-limiting and fully turbulent expressions for various flow variables. The blending functions ensure a smooth transition between the two layers and provide accurate conditions for the first cell even if it lies in the buffer region. Esch and Menter [5] proposed a quadratic blending of the wall shear stress to provide adequate boundary conditions for the $k-\omega$ model. Popovac and Hanjalić [6] developed a compound wall treatment (CWT) that reduces to either the "Integration to the wall" (ItW) or the "Wall function" approach, depending on the location of the first near-wall cell. Basara [7], followed by Rahman and Siikonen [8], used the same blending method and attempted to improve the prediction of the production and the dissipation rate.

The present study focuses on a new algebraic adaptive wall treatment for the Elliptic Blending Reynolds Stress Model (EB-RSM) by extending some of those recently proposed approaches. Blending functions that ensure a correct asymptotic behaviour at the wall for the velocity and the turbulent variables are introduced and boundary conditions are prescribed at the first near-wall cell. The approach shows very promising results on fully developed channel flows, comparable to what is obtained using a numerical integration down to the wall.

## 2 The EB-RSM for ItW

Adaptive Wall Treatment requires the use of a turbulence model integrable down to the wall. As attention is directed towards Second Moment Closures, the EB-RSM [9] is chosen. It is a robust model able to reproduce the near-wall physics. The transport equations for the turbulent variables are

$$\frac{D\overline{u_iu_j}}{Dt} = P_{ij} + \Phi^*_{ij} - \varepsilon_{ij} + D^\nu_{ij} + D^T_{ij}, \quad (1)$$

$$\frac{D\varepsilon}{Dt} = \frac{C^*_{\varepsilon_1}P - C_{\varepsilon_2}\varepsilon}{\tau} + D^\nu_\varepsilon + D^T_\varepsilon, \quad (2)$$

where $P_{ij}$ is the exact production term, the turbulent diffusion term is expressed using the Daly-Harlow model and the redistribution $\Phi^*_{ij}$ and dissipation $\varepsilon_{ij}$ terms are expressed as a blending of models valid in the fully turbulent and the wall regions,

$$\Phi^*_{ij} = (1-\alpha^3)\Phi^h_{ij} + \alpha^3\Phi^w_{ij}, \quad (3)$$

$$\varepsilon_{ij} = (1-\alpha^3)\frac{\overline{u_iu_j}}{k}\varepsilon + \frac{2}{3}\alpha^3\varepsilon\delta_{ij}, \quad (4)$$

where the superscript $h$ denotes the homogeneous part, taken from Speziale, Sarkar and Gatski [10] and $w$ the wall part, as proposed by Manceau and Hanjalić [9]. The elliptic equation solved for the blending parameter $\alpha$ is

$$\alpha - L^2\nabla^2\alpha = 1. \quad (5)$$

Finally, the integral time scale and length scale are

given by

$$L = C_L \max\left(\frac{k^{3/2}}{\varepsilon}, C_\eta \frac{\nu^{3/4}}{\varepsilon^{1/4}}\right),$$
$$\tau = \max\left(\frac{k}{\varepsilon}, C_T\sqrt{\frac{\nu}{\varepsilon}}\right). \quad (6)$$

The so-called $E$ term in the $\varepsilon$ equation, proposed by Jones and Launder (1972) and originally introduced used in the EB-RSM [9], is replaced, for numerical stability reasons, by a variable $C^*_{\varepsilon_1}$ coefficient of the form [17]

$$C^*_{\varepsilon_1} = C_{\varepsilon_1}\left(1 + A_1(1-\alpha^3)\frac{P}{\varepsilon}\right). \quad (7)$$

The original values of the coefficients of the SSG are used. Other coefficients are

| $C_\eta$ | $C_L$ | $C_T$ | $A_1$ | $C_{\varepsilon_2}$ | $C_{\varepsilon_1}$ |
|---|---|---|---|---|---|
| 80.0 | 0.122 | 6.0 | 0.1 | 1.83 | 1.44 |

## 3 Adaptive Algebraic Wall Treatment

**Velocity U**

Low-Reynolds number formulations are relevant as long as the first node is located in the viscous sublayer ($y^+ \leq 5$). However, when this point is in the fully turbulent region ($y^+ \geq 30$), natural boundary conditions become inappropriate and the use of wall functions is unavoidable. The principle of Adaptive Wall Treatment (AWT) is to provide wall boundary conditions valid whatever the first node location [6] [8]. Continuous laws for all the variables are then necessary and can be obtained, for example, by blending the viscous region (noted $F_w$) and the fully turbulent behaviour ($F_{log}$).

Many analytical laws of the wall valid throughout the whole boundary layer were proposed, starting from the pioneering work of Reichardt [11] and Spalding [12]. Although they fit perfectly experimental data, none of them would be applicable to non equilibrium flows. More recently Popovac and Hanjalić proposed such a law using Kader's blending [6].

The natural boundary conditions at a wall $u = v = 0$ and $\partial v/\partial y = 0$ lead to the asymptotic behaviour for $u$ and $v$

$$\begin{cases} u = & a_1 y + a_2 y^2 + O(y^3) \\ v = & b_2 y^2 + O(y^3) \end{cases}$$

Without any hypothesis, the asymptotic behaviour of $\overline{uv}^+$ can then be expressed as $\overline{uv}^+ = \overline{a_1 b_2} y^{+3} + O(y^{+4})$. Since $\overline{uv}$ is virtually independent of the friction Reynolds number $Re_\tau$, as confirmed by available channel flow DNS data [13, 14], $\overline{a_1 b_2}$ is assigned hereafter the constant value $\overline{a_1 b_2} = C_{\overline{uv}} = 1.0674 \times 10^{-3}$.

Introducing the expansion of $\overline{uv}^+$ in the streamwise momentum equation of a 1D channel flow at equilibrium leads to the asymptotic behaviour for $U^+$

$$U^+ = y^+ - \underbrace{\frac{y^{+2}}{2Re_\tau}}_{\Delta_2(y^+)} - \underbrace{\frac{C_{\overline{uv}}}{4} y^{+4}}_{\Delta_4(y^+)} + O(y^{+5}). \quad (8)$$

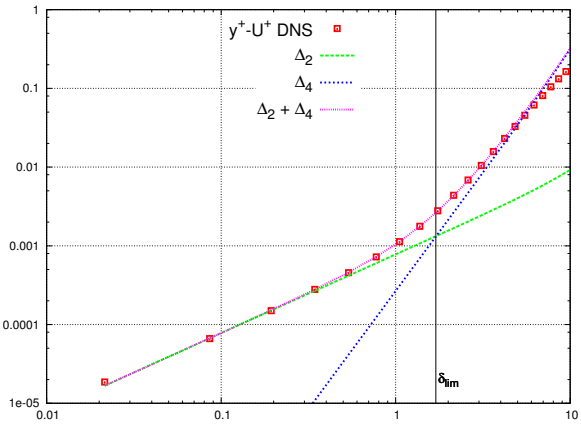


Figure 1: Comparison of the terms of the asymptotic development of $U^+$,DNS at $Re_\tau = 640$ [15]

Here, a twofold objective is aimed at:

(i) deriving a near-wall law whose validity extends further to the wall than the leading order approximation $U^+ = y^+$;

(ii) proposing a "universal" law for $U^+$, i.e., preserving its independence of the friction Reynolds number.

It then important to compare the weight of the higher order terms ($\Delta_2$ and $\Delta_4$) in equation (8).

The profile of $(U^+ - y^+)$ is extracted from the DNS data of Kasagi [15]. This data, normalized by $U^+$, represent the relative contribution of the nonlinear terms in the Taylor series expansion of $U^+$ at the wall. Fig. 1 shows that this contribution is negligible for $y+ < 5$, such that $U^+ = y^+$ is a good approximation. Beyond $y^+ = 5$, as long as $\Delta_2 + \Delta_4$ is close to $y^+ - U^+$, higher order terms ($O(y^+5)$) remain negligible. An interesting feature is that, the separate contributions of $\Delta_2$ and $\Delta_4$ to $y^+ - U^+$ are dominant in different regions: below $y^+ = \delta_{lim}$, the term of order 2, $\Delta_2$, is dominant, but in this region, $y^+ - U^+$ is very small (the linear approximation is accurate), such that the contribution of $\Delta_2$ to $U^+$ is below 0.3%; above $y^+ = \delta_{lim}$, $\Delta_4$ is the dominant nonlinear term, and gradually becomes significant beyond $y^+ = 5$.

Two conclusions can be drawn from this analysis:

(i) Since it represents a minor part of $U^+$ when $y^+ < \delta_{lim}$ and is dominated by $\Delta_4$ when $y^+ > \delta_{lim}$, the term $\Delta_2$, which depends on $Re_\tau$, can be neglected everywhere.

(ii) Taking into account the term $\Delta_4$ extends the validity of the polynomial approximation of $U^+$ without introducing a dependence in $Re_\tau$.

Consequently, the following blended law is proposed:

$$\begin{aligned} U^+ &= f_u F_w + (1-f_u)F_{log}, \\ f_u(y^+) &= \exp\left(-\frac{C_{\overline{uv}}}{4}y^{+3}\right), \end{aligned} \tag{9}$$

where $F_w(y^+) = y^+$. The introduction of the term $\Delta_4/y^+$ in the exponential function yields the asymptotic behaviour of $U^+$ at the wall

$$U^+ = y^+ - \frac{C_{\overline{uv}}}{4}y^{+4} + O(y^{+5}), \tag{10}$$

which is Eq. (8) in which the Reynolds number dependent term, $\Delta_2$, is neglected.

The blending function being defined, one could be tempted to use for $F_{log}$ the standard log law. However, Eq. (9) can be recast as

$$f_u = \frac{U^+ - F_{log}}{F_w - F_{log}} \tag{11}$$

Since they cross at $y^+ = 11$, using the linear law for $F_w$ and the standard log law for $F_{log}$ requires the use of a blending function $f_u$ singular at this location. This problem can be circumvented by using

$$\begin{aligned} F_{log}(y^+) &= d_u(y^+)\left[\frac{1}{\kappa}\ln(y^+) + B\right], \\ d_u(y^+) &= 1 - \exp\left[-\left(\frac{y^+}{y_0}\right)^n\right] \end{aligned} \tag{12}$$

where $y_0 = 14.5$ and $n = 2.25$. The introduction of the damping function $d_u$ in front of the standard log law gets rid of the intersection of $F_w$ and $F_{log}$, thus avoiding the singularity. Figure 2 compares the proposed law with standard ones, as well as the blended law proposed by Popovac and Hanjalić[6]. It is clearly seen, in particular focusing on the velocity gradient, that the present proposal, by accounting for higher order terms in the Taylor series expansion of $U^+$ at the wall, significantly improves the reproduction of the profiles in the buffer layer.

**Reynolds Stresses $\overline{u_i u_j}$**

Instead of solving the Reynolds stress equations in the near-wall cell and imposing a boundary condition at the cell face adjacent to the wall, it is proposed here to impose the components of the Reynolds stress tensor $\overline{u_i u_j}$ in the first cell evaluated from an Algebraic Stress Model derived from the EB-RSM (EB-ASM [16]). When used in the whole domain, the EB-ASM model solves equations for $k$, $\varepsilon$ and $\alpha$, and evaluated the Reynolds stresses by locally solving a system of algebraic equations.

This system is derived from Eq. (1), by introducing the anisotropy tensor $b_{ij} = \overline{u_i u_j}/(2k) - \delta_{ij}/3$ and by using the weak equilibrium hypotheses,

$$\frac{Db_{ij}}{Dt} = 0, \tag{13}$$

$$\frac{D^\nu_{ij} + D^T_{ij}}{D^\nu_{kk} + D^T_{kk}} = \frac{\overline{u_i u_j}}{\overline{u_k u_k}}, \tag{14}$$

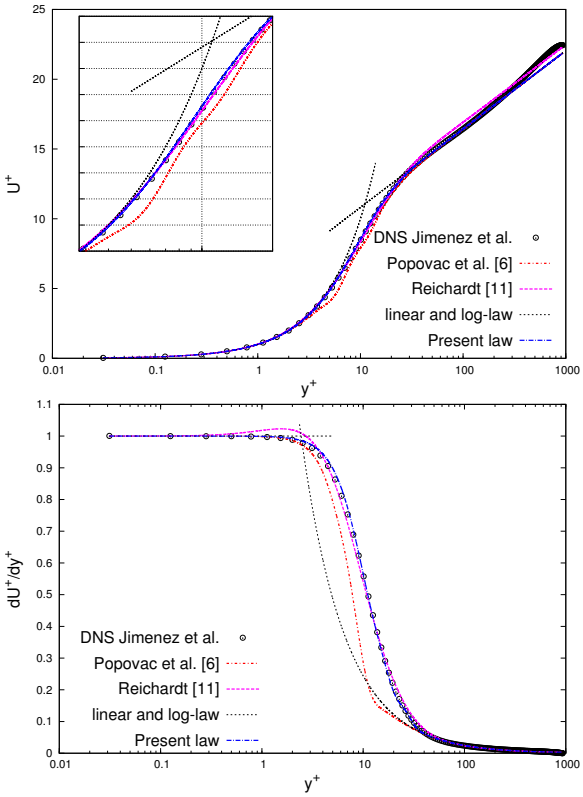


Figure 2: Comparison of the present law with that of Popovac et al.[6] and Reichardt, at $Re_\tau = 950$ [14]

which yields an algebraic system of equations for the anisotropy tensor

$$\begin{aligned} -\frac{1}{a_4}\mathbf{b} - a_3\left(\mathbf{bS} + \mathbf{Sb} - \frac{2}{3}\{\mathbf{bS}\}\mathbf{I}\right) \\ + a_2\left(\mathbf{Wb} - \mathbf{bW}\right) \\ - a_5\left(\mathbf{bM} + \mathbf{Mb} - \frac{2}{3}\{\mathbf{bM}\}\mathbf{I} - \frac{1}{2}\{\mathbf{bM}\}\mathbf{M}\right) \\ = a_1\mathbf{S} + \frac{a_5}{2}\mathbf{M}, \end{aligned} \tag{15}$$

where $\mathbf{S}$ and $\mathbf{W}$ are the mean strain and mean rotation rate tensors, respectively. They are given by the velocity law described in (9) and illustrated in figure 2. $\mathbf{M}$ is the deviatoric part of a "wall normal tensor" [16]

$$M_{ij} = n_i n_j - \frac{1}{3}\delta_{ij} \tag{16}$$

where $\mathbf{n}$ is the wall normal vector. Coefficients $a_k$ are functions of $\alpha$, $k$, $\varepsilon$, $P$ and the constants used in the

EB-RSM:

$$
\begin{aligned}
a_1 &= \frac{2}{3} - \frac{1}{2}\left(C_3 - C_3^*\sqrt{II}\right)\alpha^3 \\
a_2 &= 1 - \frac{1}{2}C_5\alpha^3 \\
a_3 &= 1 - \frac{1}{2}C_4\alpha^3 \\
a_4 &= g\tau \\
a_5 &= \frac{5}{\tau}(1-\alpha^3) \\
g &= \left[\left(1 + \frac{C_1^*}{2}\alpha^3\right)\frac{P}{\varepsilon} + \left(\frac{13}{3} - \frac{C_1}{2}\right)\alpha^3 + \frac{10}{3}\right]^{-1} \\
\tau &= \frac{k}{\varepsilon}
\end{aligned}
\tag{17}
$$

The non linear term $\sqrt{II} = \sqrt{b_{kl}b_{kl}}$ involved in the coefficient $a_1$ is treated explicitly, i.e., evaluated at the previous iteration. At each time step, the resolution of this system at the first near wall node provides all the components of the anisotropy tensor. Given the anisotropy at the first near-wall cell, it is then possible, if appropriate boundary conditions are defined for all the other turbulent variables involved in this system (the turbulent kinetic energy $k$, the dissipation rate $\varepsilon$, the production $P$ and the parameter $\alpha$), to obtain the Reynolds stress, to be imposed in the resolution of equation (1).

**Dissipation** $\varepsilon$

The same principle as for the velocity is used for the dissipation rate. $\varepsilon$ is fixed at the first near-wall cell using a blending function, which blends the near wall and fully turbulent standard behaviour as

$$
\varepsilon = f_\varepsilon\left[2\nu\frac{k}{y^2}\right] + (1-f_\varepsilon)d_\varepsilon\left[\frac{u_\tau^3}{\kappa y}\right] \tag{18}
$$

with $d_\varepsilon$ and $f_\varepsilon$ blending functions of $y^+$ only, constructed as (9), where $d_\varepsilon$ plays the same role as $d_u$ in the velocity law,

$$
\begin{aligned}
f_\varepsilon(y^+) &= \exp\left(-\left(\frac{y^+}{7}\right)^{3/2}\right), \\
d_\varepsilon(y^+) &= 1 - \exp\left(-\left(\frac{y^+}{10.5}\right)^{3/2}\right).
\end{aligned}
\tag{19}
$$

It is to be noted that this law is chosen in order to closely fit the wall-resolved EB-RSM results rather than DNS data, since the objective is to correctly reproduce behaviour of the model in the buffer layer.

**Parameter** $\alpha$

In order to identify a wall law for the elliptic blending parameter $\alpha$, it is useful to remark that, for the case of a constant length scale $L$, the analytical solution of Eq. (5) is

$$
\alpha = 1 - \exp\left(-\frac{y^+}{L}\right). \tag{20}
$$

Although $L$, modelled by Eq. (6), is not a constant, using a linearly variable $L$ in this equation, under the form

$$
\alpha = 1 - \exp\left(-\frac{y^+}{16.5 + 0.04y^+}\right), \tag{21}
$$

leads to an excellent approximation of $\alpha$, as can be seen in Fig. 4 that compares this analytical law with the parameter $\alpha$ obtained from an *a priori* channel flow analysis.

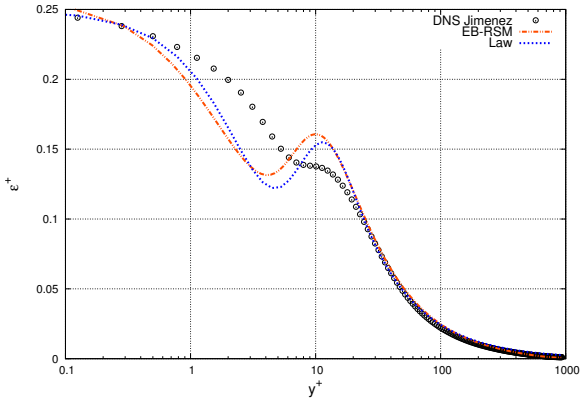


Figure 3: Comparison of the $\varepsilon$ blended law with a full EB-RSM resolution and DNS at $Re_\tau = 950$ [14]

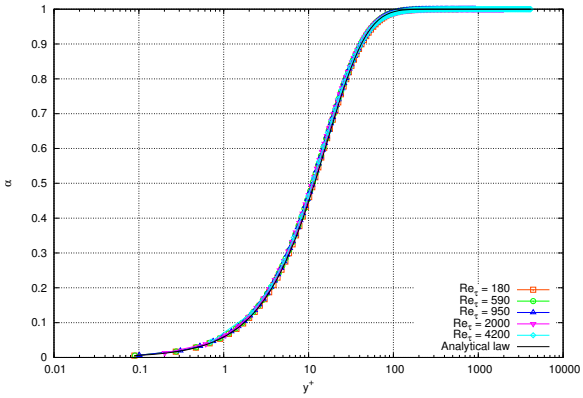


Figure 4: Comparison of the analytical law (21) with the blending parameter $\alpha$ extracted from DNS data for various Reynolds numbers.

**Turbulent Kinetic Energy** $k$

In order to compute the Reynolds stresses from the anisotropy tensor via Eq. (15), it is necessary to evaluate the turbulent energy $k$ independently of the Reynolds stresses. For this purpose, the eddy viscosity hypothesis is introduced,

$$
\nu_t = f_\mu k^2/\varepsilon, \tag{22}
$$

which yields an expression for turbulent production

$$
P = f_\mu \frac{k^2}{\varepsilon}\left(\frac{dU}{dy}\right)^2. \tag{23}
$$

Introducing expression (19) for $\varepsilon$ in this equation yields the local second order polynomial equation for

$k$

$$k^2 - \left[\frac{2\nu P f_\varepsilon}{f_\mu \left(\frac{dU}{dy}\right)^2 y^2}\right] k - \left[P d_\varepsilon (1-f_\varepsilon)\frac{u_\tau^3}{\kappa y}\right] = 0 \quad (24)$$

In order for this equation to provide an approximation for $k$, the damping function $f_\mu$ and the kinetic energy production $P$ are required. Two analytical laws for these quantities are proposed in the following sections.

**Damping function $f_\mu$.**

Since $k$ behaves as $y^{+2}$ in the vicinity of the wall, $f_\mu$ must behave as $1/y^+$ in order to ensure the correct behaviour in $y^{+3}$ of $\overline{uv}$. Therefore, the blending function for $f_\mu$ is introduced,

$$f_\mu = f_1 \frac{C_w}{y^+} + (1-f_1) C_\mu. \quad (25)$$

An *a priori* analysis of channel flow DNS data, shown in figure 5, suggests to the following set of equations and constants :

$$\begin{aligned} f_1 &= \exp\left[-\left(\frac{y^+}{39+0.2y^+}\right)^2\right], \\ C_w &= 0.016, \\ C_\mu &= 0.09, \end{aligned} \quad (26)$$

such a way that $f_\mu$ reaches the standard value $C_\mu = 0.09$ far from the wall.

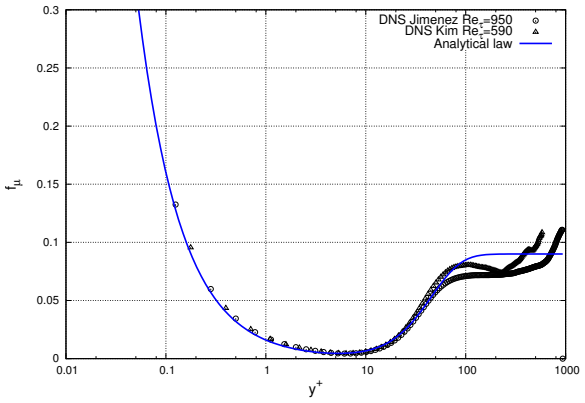


Figure 5: Comparison of the analytical law derived for $f_\mu$ with the *a priori* evaluation of $f_\mu$ from DNS data.

**Production $P$.**

Since, production writes

$$P^+ = -\overline{uv}^+ \frac{dU^+}{dy^+}, \quad (27)$$

under the assumption that the total shear remains constant from the wall up to the log layer,

$$\frac{dU^+}{dy^+} - \overline{uv}^+ = 1, \quad (28)$$

equation (27) yields

$$P^+ = \frac{dU^+}{dy^+}\left(\frac{dU^+}{dy^+} - 1\right). \quad (29)$$

The law derived above for the velocity thus provides the law for the production. Figure 6 shows very good agreement of this law with the DNS data of Hoyas and Jimenez [14], and a significant improvement compared to previous proposals.

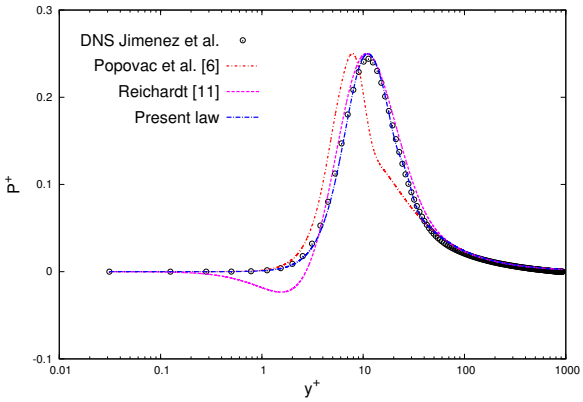


Figure 6: Comparison with the DNS data of Hoyas and Jimenez at $Re_\tau = 950$ [14] of the analytical law derived for $P^+$, using the velocity law (9)–(10)–(12), and the laws from Popovac *et al.* [6] and Reichardt [11].

**Final law for $k$.**

Using these laws for $f_\mu$ and $P$, Eq. (24) can be solved to obtain $k$. It can be seen in Fig. 7 that the profile of $k^+$ in the wall region is correctly reproduced, and the standard asymptote $k = 1/\sqrt{C_\mu}$ is recovered far from the wall. However, some small wiggles appearing in the blended law for $U^+$ are amplified by spatial derivation and are observed near the peak of $k$. Although this weakness is of minor importance in practice, future work will be devoted towards the improvement of this behaviour. It is worth emphasizing that turbulence models available in the literature, and in particular the EB-RSM, are not able to reproduce the correct sensitivity to the Reynolds number of the turbulent energy profile $k^+$. Since the wall functions developed herein are aimed at reproducing at best the results given by the underlying turbulence model in wall-resolved computations, such a dependence is not considered.

## 4 Adaptive Numerical Wall Function

As an alternative to algebraic wall functions, and following previous work of Craft *et al.* [3] (*UMIST-N* wall functions), a numerical adaptive wall treatment (NAWT) is proposed. Wherever the first calculation node is located, the one dimensional form of the EB-RSM is solved on a sub-mesh embedded in the first wall control volume. Consistently with the previous

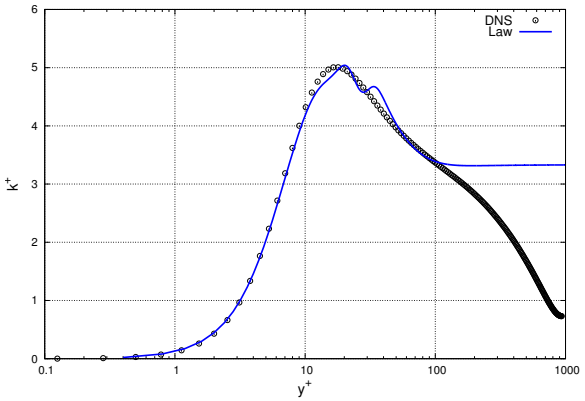


Figure 7: Comparison of the law developed for $k^+$ with DNS data of Hoyas and Jimenez at $Re_\tau = 950$ [14].

algebraic strategy, the value of the variables are then imposed in the first cell. This strategy is schematically described in figure 8. One can notice that with a 1D

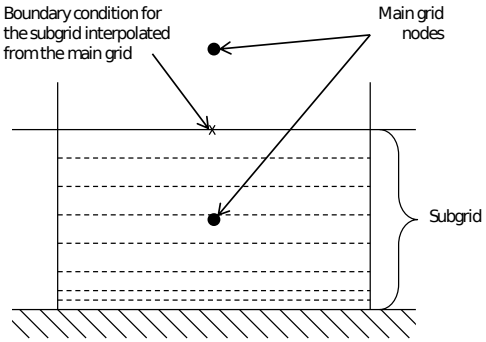


Figure 8: Arrangement of the subgrid in the near wall cell.

assumption between the first calculation node and the wall, we cannot obtain better results than the ones obtained with this approach.

## 5 Results

Both the numerical (NAWF) and algebraic (AAWF) approaches described above are tested in several fully developed channel flows. Figures 9, 10 and 11 show the results for different locations of the first near wall cell ($y^+ = 1, 5, 10, 30, 50$) at $Re_\tau = 590$, in comparison with the DNS data of Moser *et al.* [13]. For all meshes, the obtained profiles agree very well with the reference data. The most notable difference obtained in these computations is the presence of a kink in the profiles of the variables, mostly when the first point lies in the buffer layer. This is not due to the wall functions themselves, but rather to the coarse discretization of the transport equations in the few coarse cells adjacent to the first cell: this discretization error vanishes with refinement, i.e., when all the cells

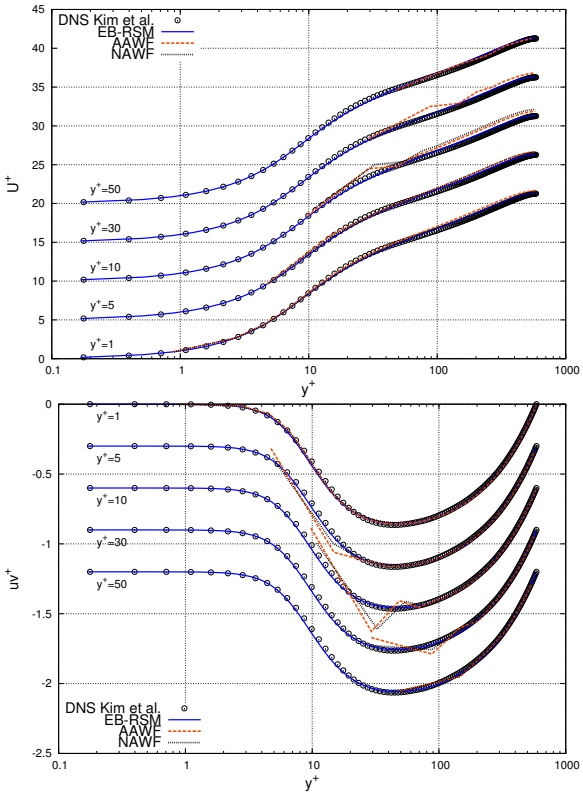


Figure 9: Prediction of $U^+$ and $\overline{uv}^+$

but the first one are refined (not shown here). Figure 12 presents the velocity for three different turbulent Reynolds number at three different locations for the AAWF approach and confirms the quality of the results.

The behaviour of the law in the buffer layer is particularly satisfactory. The exposed strategy can indeed reproduce the bump of the dissipation rate and shows very good prediction of the turbulent kinetic energy and the mean velocity around $y^+ = 10$. It can be seen that both strategies show equivalent results in this channel flow configuration. It is however expected that, in non equilibrium configurations, the integration over a subgrid (NAWF) will lead to better agreement with experimental data [3], such that future work will be devoted to the introduction of non-equilibrium effects in the analytical algebraic wall functions.

## 6 Conclusions

Adaptive wall functions for the EB-RSM, based on either algebraic relations or a numerical 1D integration, are introduced. They are applicable whatever the position of the first cell centre and show good agreement with the wall-resolved EB-RSM results for all the variables on channel flow configurations. Further work is in progress to make these wall functions sensitive to pressure gradient and streamwise acceleration effects, in order to address more complex validation

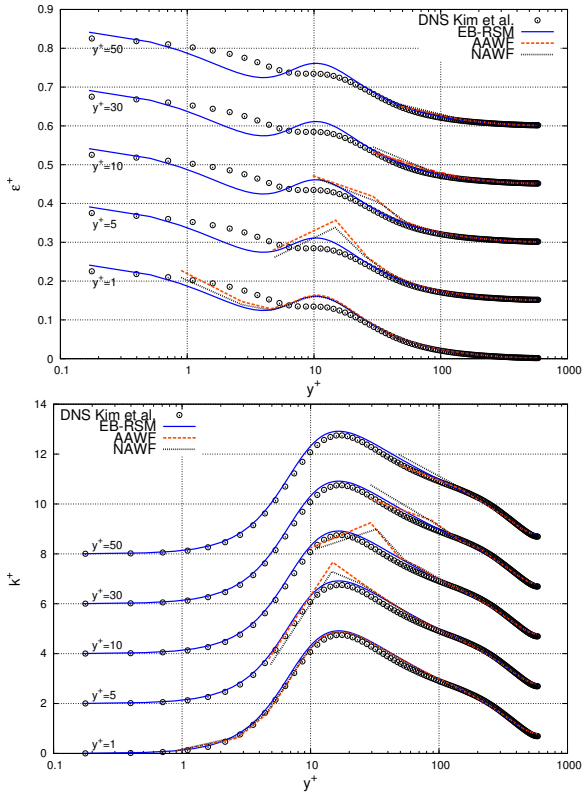


Figure 10: Prediction of $k^+$ and $\varepsilon^+$

test cases.

## References


[1] Chieng CC, Launder BE, 1980, On calculation of turbulent heat transport downstream from an abrupt pipe expansion, *Numer. Heat Transfer*, Vol. 3, pp. 189207

[2] T.J. Craft, A.V. Gerasimov, H. Iacovides, B.E. Launder, 2002, Progress in the generalisation of wall function treatment, *Int. J. Heat Fluid Flow*, Vol. 23, pp. 148-160.

[3] T.J. Craft, S.E. Gant, H. Iacovides and B.E. Launder, 2004, A new wall function strategy for complex turbulent flows, *Numer. Heat Transfer, B*, Vol. 45, pp. 301-317.

[4] G. Kalitzin, G. Medic, G. Iaccarino, P. Durbin, 2005, Near-wall behaviour of RANS turbulence models and implications for wall functions, *J. Comput. Phys.*, Vol. 420, pp. 265-291

[5] T. Esch and F.R. Menter , 2003,Heat transfer predictions based on two-equation turbulence models with advanced wall treatment, *Turbu. Heat Mass Transf.*, Vol. 4, pp. 633-640

[6] M. Popovac and K. Hanjalić, 2007, Compound wall treatment for RANS computation of complex turbulent flows and heat transfer, *Flow Turb. Comb.*, Vol. 78, pp. 177-202.

[7] B. Basara, 2006, Eddy viscosity transport model based on elliptic relaxation approach, *AIAA Journal*, Vol. 44, pp. 16861690

[8] M.M. Rahman and T. Siikonen, 2012, Compound wall treatment with low-Re turbulence model, *Int. J. Numer. Meth. Fluids*, Vol. 68, pp. 706-723.

[9] R. Manceau and K. Hanjalić, 2002, Elliptic blending model : A new near-wall Reynolds-stress turbulence clo-


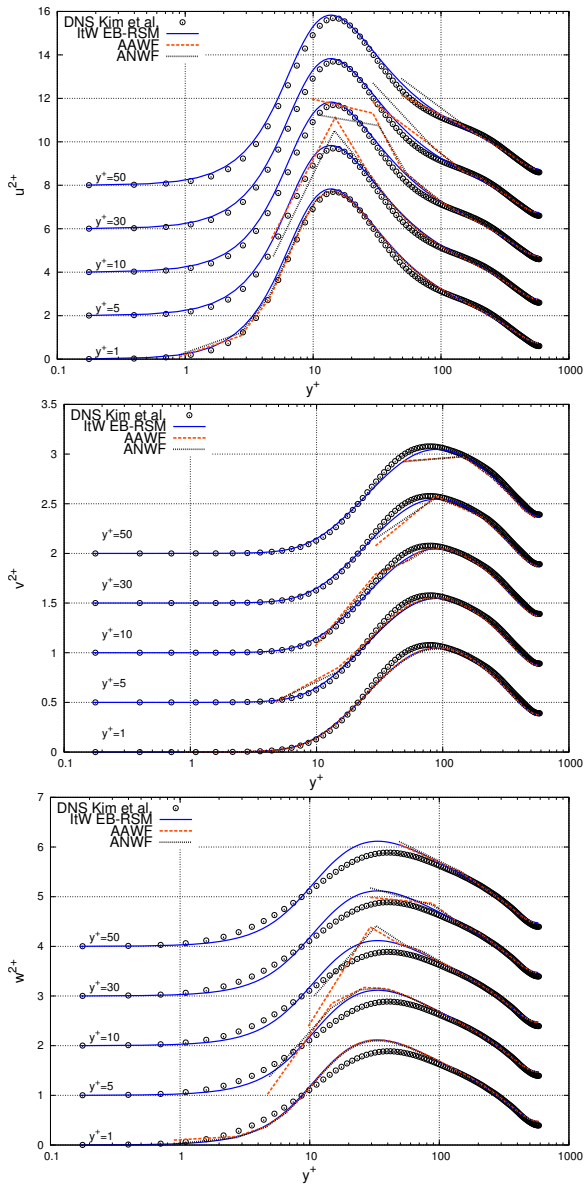


Figure 11: Prediction of $\overline{u^2}$,$\overline{v^2}$ and $\overline{w^2}$

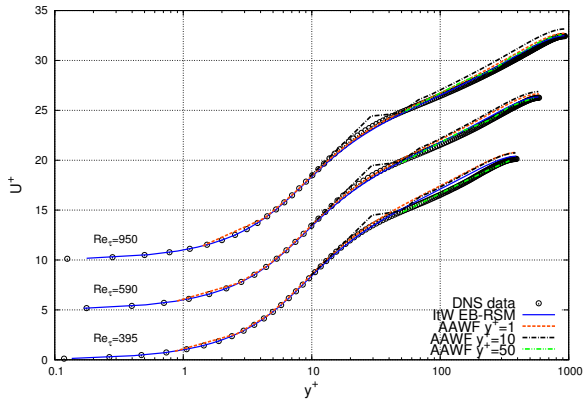


Figure 12: Velocity $U^+$, compared with DNS of Moser *et al.* [13] and Hoyas and Jimenez [14]

sure, *Phys. of Fluids*, Vol. 14, pp. 744-754.

[10] C. G. Speziale, S. Sarkar, and T. B. Gatski, 1991, Modeling the pressurestrain correlation of turbulence: an invariant dynamical system approach, *J.Fluid Mech.*, Vol. 227, pp. 245

[11] H. Reichardt, 1951, Vollstandige Darstellung der turbulenten Geschwindigkeitsverteilung in glatten Leitungen, *Z. angew. Math. Mech.*, Vol. 31, pp. 208219

[12] D. B. Spalding, 1961, A Single Formula for the Law of the Wall , *J. Appl. Mech.*, Vol. 28, pp. 455-458.

[13] R. D. Moser, J. Kim and N. N. Mansour, Direct numerical simulation of turbulent channel flow up to $Re_\tau = 590$, *Phys. of Fluids*, Vol. 11, pp. 943-945.

[14] S. Hoyas and J. Jimenez, 2006, Scaling of velocity fluctuations in turbulent channels up to $Re_\tau = 2000$", *Phys. of Fluids*, Vol. 18, 011702.

[15] Iwamoto, K., Suzuki, Y., and Kasagi, N., 2002, Reynolds Number Effect on Wall Turbulence: Toward Effective Feedback Control, *Int. J. Heat and Fluid Flow*, Vol. 23, pp. 678-689.

[16] A.G. Oceni, Modélisation algébrique explicite à pondration elliptique pour les écoulements turbulents en présence de paroi, 2009, *PhD Thesis*.

[17] F. Dehoux, Y. Lecocq, S. Benhamadouche, R. Manceau and L.-E. Brizzi, 2012, Algebraic modeling of the turbulent heat fluxes using the elliptic blending approach. Application to forced and mixed convection regimes, *Flow Turbul. Combust.*, Vol. 88, pp. 77-100.